CSIRO PUBLISHING
www.publish.csiro.au/journals/pasa *Publications of the Astronomical Society of Australia*, 2009, **26**, 243–249

Neutron Capture Cross Sections for the Weak *s* Process

M. Heil[A,G], *A. Juseviciute*[B], *F. Käppeler*[B], *R. Gallino*[C,D], *M. Pignatari*[E,F], *and E. Uberseder*[F]

[A] Gesellschaft für Schwerionenforschung (GSI), D-64291 Darmstadt, Germany
[B] Forschungszentrum Karlsruhe, Institut für Kernphysik, D-76021Karlsruhe, Germany
[C] Dipartimento di Fisica Generale, Università di Torino, Via P. Giuria 1, 10125 (Torino), Italy
[D] Center for Stellar and Planetary Astrophysics, Monash University, Victoria 3800, Australia
[E] Astrophysics Group, School of Physical and Geographical Sciences, Keele University, UK
[F] Joint Institute for Nuclear Astrophysics, University of Notre Dame, Notre Dame, IN 46556, USA
[G] Corresponding author. Email: m.heil@gsi.de

Received 2008 December 14, accepted 2009 March 3

Abstract: In past decades a lot of progress has been made towards understanding the main *s*-process component that takes place in thermally pulsing Asymptotic Giant Branch (AGB) stars. During this process about half of the heavy elements, mainly between $90 \leq A \leq 209$ are synthesized. Improvements were made in stellar modeling as well as in measuring relevant nuclear data for a better description of the main *s* process. The weak *s* process, which contributes to the production of lighter nuclei in the mass range $56 \leq A \leq 90$ operates in massive stars ($M \geq 8\,\mathrm{M}_\odot$) and is much less understood. A better characterization of the weak *s* component would help disentangle the various contributions to element production in this region. For this purpose, a series of measurements of neutron-capture cross sections have been performed on medium-mass nuclei at the 3.7-MV Van de Graaff accelerator at FZK using the activation method. Also, neutron captures on abundant light elements with $A < 56$ play an important role for *s*-process nucleosynthesis, since they act as neutron poisons and affect the stellar neutron balance. New results are presented for the (n, γ) cross sections of ^{41}K and ^{45}Sc, and revisions are reported for a number of cross sections based on improved spectroscopic information.

Keywords: stars: AGB — nuclear reactions, nucleosynthesis, abundances

1 Introduction

Since 1957, after the pioneering work by Burbidge et al. (1957), it is known that the elements heavier than iron are mainly produced by two neutron capture processes, the slow (*s*) and the rapid (*r*) process, both contributing about half of the observed solar abundances between Fe and U. A third process, the so called photodissociation *p* process is responsible for the origin of about 30 rare, proton-rich nuclei, but does not contribute significantly to the synthesis of the elements in general (<1%).

The main *s* process produces predominantly nuclei with mass numbers $A > 90$ and is by far the most studied process. In recent years, a detailed stellar model was developed (Straniero et al. 1995) which suggests that the main component of the *s* process occurs in the He-rich intershell of thermally pulsing (TP) AGB stars and the calculated *s* abundances are in excellent agreement with observations (Arlandini et al. 1999).

The weak *s* component, on the other hand, is much less understood. It is responsible for the production of nuclei between iron and strontium ($56 \leq A \leq 90$). Current stellar models suggest that it takes place during convective core-He burning in massive stars ($M \geq 8\,\mathrm{M}_\odot$), where temperatures of $(2.2–3.5) \times 10^8$ K at the center are reached near He exhaustion and neutrons are liberated by the activation of the ^{22}Ne$(\alpha, n)^{25}$Mg reaction. Since the neutron exposure is small, the *s*-process flow can not overcome the bottleneck at the closed neutron shell $N = 50$. Most of the material is reprocessed by the following burning stages and only a small part survives in the outer layers of the previous convective core He burning and is ejected during the supernova explosion. A second neutron exposure occurs during convective carbon shell burning of massive stars (Raiteri et al. 1993; Rauscher et al. 2002; The, El Eid & Meyer 2007). There, neutrons are produced mainly by burning leftover ^{22}Ne. Since ^{22}Ne derives from initial CNO nuclides, first converted to ^{14}N by H burning and then by the chain $^{14}\mathrm{N}(\alpha, \gamma)^{18}\mathrm{F}(\beta\nu)^{18}\mathrm{O}(\alpha, \gamma)^{22}\mathrm{Ne}$ occurring in the first phase of core He burning, the weak-*s* yields decrease with metallicity. The high temperatures during carbon burning of $T \sim 1 \times 10^9$ K cause high neutron densities up to $\sim 10^{12}\,\mathrm{cm}^{-3}$.

The nucleosynthesis yields of the weak component in massive stars are also important for *r*-process supernova scenarios, since they determine the composition of a star before the supernova explosion. Since the *s*-process abundances can be determined reliably on the basis of experimental (n, γ) cross sections, the *r* abundances

© Astronomical Society of Australia 2009 10.1071/AS08064 1323-3580/09/03243

https://doi.org/10.1071/AS08064 Published online by Cambridge University Press

are commonly inferred by the *r*-residual method, that is by subtracting the *s* abundances from solar values, $N_r = N_\odot - N_s$ (Anders & Grevesse 1989). The *r* abundances obtained in this way are then used for testing *r*-process models. This is of special interest, since recent observations of ultra-metal-poor halo stars (Sneden et al. 2003) suggest a second, so-called weak *r* process, which contributes to the element production below barium.

In addition, current *s*-process models cannot explain the high observed abundances of the typical *s* elements Sr, Y and Zr in halo stars with low metallicity (Travaglio et al. 2004). Since the *s* process is a secondary process, significant contributions are expected only for metallicities [Fe/H] > -1.5. Therefore, a new primary neutron capture process, the lighter element primary process (LEPP) was suggested by Travaglio et al. (2004). Another scenario pointing to an *s*-process origin of LEPP is that this extra component is produced by fast rotating metal-poor massive stars. The rotation mixes primary ^{14}N in the He core where it is converted into primary ^{22}Ne, causing a strong production of neutrons before the He exhaustion and in the following C shell (Pignatari et al. 2008).

Recently, a totally new process, the νp process, was introduced (Fröhlich et al. 2006), where nucleosynthesis calculations explored the, so far, neglected effect of neutrino interactions and found that it is possible to produce neutrons via antineutrino captures on protons in the innermost proton-rich ejecta of core-collapse supernovae. Neutron densities of 10^{14}–10^{15} cm^{-3} could be obtained in this way for several seconds, when the temperatures are in the range 1–3 GK.

It is clear from the above discussion that several processes contribute to the nucleosynthesis of medium-heavy nuclei from Fe to Ba. In order to disentangle the various processes and to identify possible astrophysical sites, the individual contributions have to be separated. A first step could be the identification of the abundance contributions from the weak *s* process, since the most important nuclear data input, the neutron capture cross sections, are accessible by laboratory experiments. Therefore, new measurements of neutron-capture cross sections of medium-mass nuclei are demanded.

The cross sections of light elements are also important in this respect because they affect the neutron balance inside stars during the *s* process. Although their cross sections are small, these elements are much more abundant than those in the mass region above Fe. Therefore, light elements constitute potential neutron poisons and may consume neutrons, which are then not available for *s*-process nucleosynthesis. Especially important in this respect are neutron captures on ^{12}C, ^{16}O and on the neon and magnesium isotopes, but other light isotopes up to iron contribute as well. In many of these cases the neutron capture cross sections are not known with sufficient accuracy since they are small and difficult to measure.

Neutron-capture cross sections of light isotopes play also an important role for analyses of pre-solar grains, which can provide stringent constraints on *s*-process models (Zinner 1998). Because these grains are only a few μm in size and because the abundances of heavy elements are rather low, their isotopic composition is difficult to determine for individual grains. Lighter elements are more abundant and, therefore, easier to detect.

In this contribution we report on neutron-capture cross section measurements of ^{41}K and ^{45}Sc. The experimental method and the results are described in Section 2. The measurements are part of a series of neutron capture studies on light and medium heavy nuclei relevant for the weak *s* process in massive stars, which will be summarized in Section 3. Section 4 concludes with some remarks on the astrophysical implications of these results.

2 Activation Method

The most important input for stellar models of the *s* process are Maxwellian averaged neutron-capture cross sections (MACS) and β-decay rates, but also stellar enhancement factors (SEF) have to be known.

The weak *s* process contributes substantially to the production of elements in the mass range $56 \leq A \leq 90$. In this mass region the (n, γ) cross sections show large uncertainties and need significant improvement for a reliable description of the abundance contributions from massive stars. This is especially important since the local approximation ($\langle\sigma\rangle N = \text{const}$) is not valid during the weak *s* process. Therefore, any change in the cross section of a light isotope, e.g. ^{62}Ni (Nassar et al. 2005), can affect the abundances of all the heavier isotopes up to zirconium and maybe even higher up. This underlines that neutron-capture cross sections in the mass range $50 \leq A \leq 90$ have to be measured with significantly higher accuracy.

Therefore, a measuring campaign was launched at Forschungszentrum Karlsruhe with the aim to improve the neutron-capture cross sections of light and medium-mass nuclei. A reliable and accurate approach to determine Maxwellian averaged cross sections at $kT = 25$ keV is the activation method (Beer & Käppeler 1980), where the ^{7}Li$(p, n)^7$Be reaction is used to produce a quasi-stellar neutron spectrum as sketched in Figure 1. After irradiation in that spectrum the induced sample activity is counted in a low background environment with high resolution Ge detectors. The proton beam with an energy of $E_p = 1912$ keV and typical intensities of 100 μA was

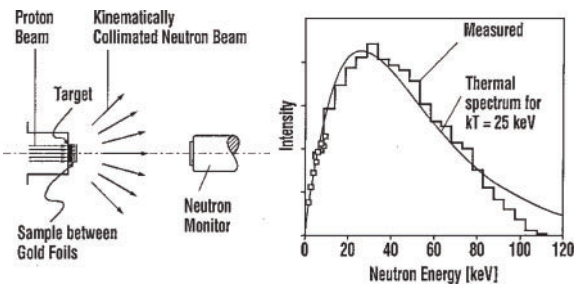

Figure 1 The experimental setup for activation measurements (left) and a comparison of the produced neutron spectrum and a thermal neutron spectrum at $kT = 25$ keV (right).

https://doi.org/10.1071/AS08064 Published online by Cambridge University Press

delivered by the Karlsruhe 3.7-MV Van de Graaff accelerator. The neutron production target consists of a metallic Li layer, which is evaporated onto a water cooled copper backing. The sample is placed inside the resulting neutron cone, which has an opening angle of 120° in the direction of the proton beam. The neutron flux is monitored throughout the irradiations by means of a ^{6}Li-glass detector, positioned at a distance of 1 m from the target. After the irradiation the total number of activated nuclei A_c is given by

$$A_c = \Phi N \sigma f_b, \tag{1}$$

where Φ is the time-integrated neutron flux, N is the number of sample atoms per cm^2, and σ the spectrum-averaged, neutron-capture cross section. In order to determine the neutron flux, the sample is sandwiched between gold foils. Since the gold cross section is well known, the total number of neutrons can be obtained by measuring the 412 keV line from the decay of ^{198}Au with HPGe detectors. The factor f_b accounts for the variation of the neutron flux and for the decay during activation. The cross section is then calculated from the number of counts in a characteristic γ-ray line

$$C_\gamma = A_c K_\gamma \varepsilon_\gamma I_\gamma (1 - e^{-\lambda t_m}) e^{-\lambda t_w}, \tag{2}$$

where K_γ is a correction factor for γ-ray self-absorption, ε_γ the efficiency of the Ge-detector, I_γ the line intensity, t_w the waiting time between irradiation and counting, and t_m the duration of the activity measurement.

In this way, we have measured the MACSs of several nuclei. As an example, we give here details of the measurements on ^{41}K, and ^{45}Sc at $kT = 25$ keV. A brief summary of all measurements follows in Section 3.

By variation of sample dimensions and other basic experimental parameters in repeated activations it was possible to verify the data analysis procedures and to check the reliability of the evaluated uncertainties of the measurements. The information on the relevant parameters of the different activation runs are given in Table 1. The decay properties of the product nuclei, which are essential for determining the induced activities are summarized in Table 2. A detailed description of the procedures used in the measurements and in data analysis can be found in Heil et al. (2008a) and references therein.

The experimental results and uncertainties are summarized in Tables 3 and 4. In spite of the variation of the experimental parameters, the results are all consistent within the estimated uncertainties, thus confirming the reliability of the experimental method. These variations included different sample sizes and masses to verify the corrections for finite size and self shielding effects as well as different irradiation times to control uncertainties due to the half-lives of the respective product nuclei. Significant contributions to the overall uncertainty originate from the gold reference cross section, the efficiency of the HPGe detectors, and the time integrated neutron flux, whereas the uncertainties from the γ-decay intensities are small.

The results in Table 3 represent cross section values averaged over the quasi-stellar neutron spectrum used for the irradiations. In order to derive MACSs which are defined as

$$\langle\sigma\rangle_{kT} = \frac{\langle\sigma v\rangle}{v_T} = \frac{2}{\sqrt{\pi}} \frac{\int_0^\infty \sigma(E_n) E_n e^{-E_n/kT} dE_n}{\int_0^\infty E_n e^{-E_n/kT} dE_n}. \tag{3}$$

We used the evaluated energy-dependent cross sections, $\sigma(E_n)$, from data libraries, which were normalized to reproduce our experimental results. In the above formula E_n denotes the neutron energy, k the Boltzmann factor, and T the temperature. The MACSs obtained for various thermal energies are listed in Tables 5 and 6 for the respective libraries as well as for the temperature trend of the compilation by Bao et al. (2000).

Since it is not obvious which trend with kT is to be preferred, and since it is beyond the scope of this paper to trace the origin of the differences between various evaluations, the recommended values (which have been used for the *s*-process calculations discussed in the following section) are the ones obtained using the temperature trend of Bao et al. (2000). This choice was motivated by the fact that

Table 1. Summary of irradiation parameters

Activation	Sample comp.	Mass (mg)	Diameter (mm)	Irrad. time (min)	Φ (10^{14})
1	KBr	98.70	6	156	0.2681
2	KBr	733.27	12	1118	0.7069
3	Sc metal	2.43	6	2829	5.019
4	Sc metal	6.37	10	4148	3.352
5	Sc metal	9.57	12	2829	1.855

Table 2. Decay properties of the product nuclei

Product nucleus	Half-life (min)	γ-Ray energy (keV)	Intensity per decay (%)	Reference
^{42}K	741.6 ± 0.72	1524.6 ± 18.08	0.09	Singh & Cameron (2001)
^{46}Sc	120658 ± 58	889.28 ± 99.984	0.001	Wu (2000)
		1120.55 ± 99.987	0.001	
^{198}Au	3881.1 ± 0.29	411.8 ± 95.6	0.12	Chunmei (2002)

https://doi.org/10.1071/AS08064 Published online by Cambridge University Press

Table 3. Measured cross sections

Activation	γ-Ray energy (keV)	Self-absorption factor	Cross section (mbarn)	Mean value (mbarn)
^{41}K$(n,\gamma)^{42}$K				
1	1524.6	0.99	$20.4 \pm 1.6 \pm 0.7$	
2		0.98	$20.2 \pm 0.5 \pm 0.6$	20.3 ± 0.8(stat) ± 0.7(sys)
^{45}Sc$(n,\gamma)^{46}$Sc				
3	889.28	1.00	$59.3 \pm 0.9 \pm 1.8$	
	1120755	1.00	$61.7 \pm 1.0 \pm 1.9$	
4	889.28	1.00	$59.7 \pm 0.7 \pm 1.8$	
	1120.55	1.00	$61.0 \pm 0.7 \pm 1.8$	
5	889.28	1.00	$60.3 \pm 0.7 \pm 1.8$	
	1120.55	1.00	$60.0 \pm 0.8 \pm 1.8$	60.3 ± 0.4(stat) ± 1.8(sys)

Table 4. Compilation of systematic uncertainties

Source of uncertainty	Uncertainty (%)		
	Au	^{41}K	^{45}Sc
Gold cross section	1.5	–	–
Number of nuclei	0.6	0.1	0.4
Time factors f_b, and $t_{1/2}$	<0.1	<0.1	<0.1
Self-absorption	<1.0	<1.0	<1.0
Detector efficiency	1.5	1.5	1.5
γ-Ray intensity per decay	0.13	0.5	0.001
Neutron flux	–	2.6	2.4
Total uncertainty	–	3.2	3.0

Table 5. MACSs for the ^{41}K$(n,\gamma)^{42}$K reaction[a]

kT (keV)	JEFF 3.1[b] (mbarn)	JENDL 3.3[c] (mbarn)	Bao et al. (2000) (mbarn)
5	91.2	91.2	$75.9^{+16.3}_{-5.7}$
10	50.7	50.7	$42.5^{+8.8}_{-3.2}$
15	35.3	35.3	$30.8^{+5.1}_{-2.3}$
20	26.7	26.6	$24.8^{+2.7}_{-1.9}$
25	21.3	21.3	$21.3^{+1.6}_{-1.6}$
30	17.8	17.8	$19.0^{+1.4}_{-1.9}$
40	13.8	15.4	$16.1^{+1.2}_{-2.6}$
50	11.7	11.7	$14.4^{+1.1}_{-2.9}$
60	10.4	10.4	$13.2^{+1.0}_{-3.0}$
80	9.1	9.1	$11.6^{+0.9}_{-2.6}$
100	8.4	8.4	$10.4^{+0.8}_{-2.1}$

[a]Calculated with the normalized neutron-capture cross sections of various databases compared with the temperature trend of Bao et al. (2000).
[b]JEFF/3.1 (`www.nea.fr/html/dbdata/JEFF/`).
[c]JENDL/3.3 (`wwwndc.tokai-sc.jaea.go.jp/jendl/`).

these data include the most recent time-of-flight (TOF) results. The uncertainties of the extrapolated MACS were estimated by comparison with the upper and lower bounds obtained by using the evaluated cross sections from the data libraries. The uncertainties of the recommended values are, therefore, composed of the experimental uncertainties originating from the measured data and of the contributions defined by the differences with respect to the values derived from different databases.

Since the MACS in Tables 5 and 6 have already been normalized to the present cross section results, it is interesting to note the normalization factors as well. For ^{41}K these are 0.57, 0.57 and 0.86 for JEFF/3.1, JENDL/3.3 and Bao et al. (2000), and for ^{45}Sc 0.88, 0.85, 0.88 and 0.80 for JEFF/3.1, ENDF/B-6.8, JENDL/3.3 and Bao et al. (2000), respectively.

The present results are consistently smaller compared to previous data, which both have been obtained in TOF experiments. For the MACS of ^{41}K the only other experiment reports a 12% larger value (Macklin 1984), whereas the present and previous measurement claim uncertainties of only 3.2% and 7.5%. In case of ^{45}Sc there is also only one other experimental value (Kenny, Allen & Macklin 1977), which is 25% larger, far outside the quoted uncertainties of 7.2% and the present 3.0%.

3 Neutron-Capture Measurements

With the activation technique described before, we have determined a number of MACSs in the mass range of the weak *s* process between Fe and Zr. Apart from the measurements on ^{41}K and ^{45}Sc presented here, the results for the other isotopes in our study were published elsewhere. In order to provide an overview all recent measurements are summarized in Table 7 and compared with the previously recommended values (Bao et al. 2000).

For some isotopes the measured cross sections differ significantly from previous recommendations. It is conspicuous that many new results are systematically smaller than the recommended cross sections from Bao et al. (2000), which are often based on TOF measurements performed with C_6D_6 detectors in the 1970s and early 1980s (Kenny, Allen & Macklin 1977; Macklin 1984; Musgrove, Allen & Macklin 1978). In fact, this trend is confirmed by a general comparison between MACSs obtained with the

https://doi.org/10.1071/AS08064 Published online by Cambridge University Press

Table 6. MACSs for the ^{45}Sc(n, γ)^{45}Sc reaction[a]

kT (keV)	JEFF 3.1[b] (mbarn)	ENDF B-6.8[c] (mbarn)	JENDL 3.3[d] (mbarn)	Bao et al. (2000) (mbarn)
5	163	161	163	181^{+7}_{-21}
10	115	115	115	123^{+5}_{-9}
15	89.7	88.8	89.7	$92.9^{+3.4}_{-5.3}$
20	74.6	73.4	74.7	$76.1^{+2.8}_{-3.9}$
25	64.3	63.2	64.7	$64.1^{+2.3}_{-2.3}$
30	56.8	56.1	57.5	$55.3^{+3.0}_{-2.0}$
40	46.4	46.9	47.7	$43.3^{+4.7}_{-1.6}$
50	39.5	41.1	41.2	$35.3^{+6.0}_{-1.3}$
60	34.4	36.8	36.6	$30.4^{+6.5}_{-1.1}$
80	27.7	30.6	30.3	$24.8^{+5.9}_{-0.9}$
100	23.4	26.0	26.2	$21.6^{+4.7}_{-0.8}$

[a]Calculated with the normalized neutron-capture cross sections of various databases compared with the ones obtained using the temperature trend of Bao et al. (2000).
[b]JEFF/3.1 (`www.nea.fr/html/dbdata/JEFF/`).
[c]ENDF/B-VI.8 (`www.nndc.bnl.gov/`).
[d]JENDL/3.3 (`wwwndc.tokai-sc.jaea.go.jp/jendl/`).

Table 7. Recent MACS at $kT = 30$ keV compared with previously recommended values

Target isotope	Bao et al. (2000)	Present activations	Reference
^{19}F	5.8 ± 1.2	3.2 ± 0.1	Uberseder et al. (2007)
^{41}K	22.0 ± 0.7	$19.0^{+1.4}_{-1.9}$	This work
^{45}Sc	69 ± 5	$55.3^{+3.0}_{-2.0}$	This work
^{58}Fe	12.1 ± 1.3	$13.5^{+0.6}_{-0.8}$	Heil et al. (2008a)
^{59}Co	38 ± 4	$39.6^{+2.7}_{-2.5}$	Heil et al. (2008a)
^{64}Ni	8.7 ± 0.9	$8.0^{+0.5}_{-0.8}$	Heil et al. (2008a)
^{63}Cu	94 ± 10	$56.0^{+2.2}_{-5.2}$	Heil et al. (2008a)
^{65}Cu	41 ± 5	$30.0^{+1.3}_{-1.9}$	Heil et al. (2008a)
^{79}Br	627 ± 42	613 ± 59	Heil et al. (2008a)
^{81}Br	313 ± 16	235 ± 9	Heil et al. (2008a)
^{85}Rb	240 ± 9	221^{+13}_{-6}	Heil et al. (2008a)
^{87}Rb	15.5 ± 1.5	$15.8^{+0.7}_{-0.9}$	Heil et al. (2008a)

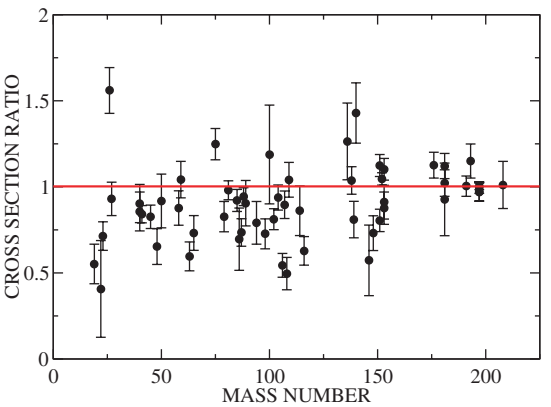

Figure 2 Comparison of MACSs at $kT = 30$ keV obtained by activation and by the TOF method. Note that most ratios are smaller than unity.

activation method and the TOF method performed with C_6D_6 detectors, which reveal large discrepancies on average. The cross sections from activation measurements are consistently lower, often in complete disagreement within the quoted uncertainties.

This is illustrated in Figure 2 by the comparison between MACSs at $kT = 30$ keV obtained with the TOF and the activation method. A possible explanation could be that the background due to sample-scattered neutrons was systematically underestimated in older TOF experiments. Neutrons scattered in the sample and captured in the detector and/or in surrounding materials produce background events, which are difficult to distinguish from true capture events. This background can be as high as 50% for light and medium heavy nuclei, where the scattering/capture ratios are large. The correspondingly large and uncertain corrections tend to give rise to large systematic errors.

It should be also noted that some activation measurements performed in the past are inconsistent with newer results. The neutron capture cross section of ^{81}Br can serve as an example. The MACS at $kT = 30$ keV of the activation measurement in 1986 of 317 ± 16 mb (Walter et al. 1986) is in contradiction to the new result of Heil et al. (2008b) of 235 ± 9 mb. Note that, in contrast to the previous result, which was measured in 1986 by a single activation, several repeated activations were performed by Heil et al. (2008b) by variation of sample dimensions and other experimental parameters as described before.

Since activation measurements have to rely on sometimes rather uncertain decay properties of the respective product nuclei, any improvement of these basic parameters such as decay intensities or half-lives are important and

https://doi.org/10.1071/AS08064 Published online by Cambridge University Press

Table 8. MACS at $kT = 30$ keV

Target isotope	Bao et al. (2000)	Corr. factor	New MACS	Ref. to new decay data
^{46}Ca	5.7 ± 0.5^{a}	1.085	6.2 ± 0.7	Burrows (1995)
	4.9 ± 0.6^{b}	1.042	5.1 ± 0.5	
^{124}Xe	644 ± 83	0.958	617 ± 79	Katakura (1999)
^{155}Eu	1320 ± 84	0.883	1166 ± 73	Reich (1994)
^{152}Gd	1030 ± 65	0.930	958 ± 47	Helmer (1998)
^{158}Gd	221 ± 25	0.816	178 ± 42	Helmer (1998)
^{160}Gd	144 ± 14	1.618	230 ± 16	Reich & Helmer (2000)

[a]Correction for value in Käppeler, Walter & Mathews (1985).
[b]Correction for value in Mohr et al. (1999).

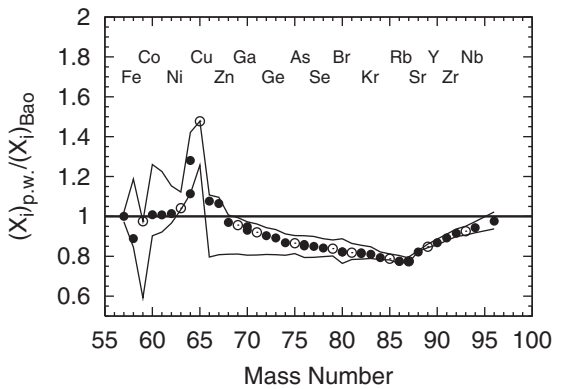

Figure 3 Nucleosynthesis yields between Fe and Nb illustrating the final *s*-process yields after shell C burning for a 25-$M_\odot$ star with [Fe/H] = 0. To illustrate the combined effect of all new cross sections the yield is plotted relative to the standard case using the cross sections of Bao et al. (2000) (p.w. stands for present work, even- and odd-*Z* elements are distinguished by black and open symbols, respectively). The thin lines correspond to the upper and lower limits of the cross sections in Tables 6 and 7 and demonstrate the uncertainties stemming from the extrapolation of the measured cross sections to higher and lower energies.

can be used for the revision of older activation data. A systematic search for improved decay information resulted in the set of updated MACSs, which are listed in Table 8 together with the corresponding correction factors and references to the new decay data.

4 Astrophysical Implications

The MACS obtained in a series of neutron capture measurements with the activation method have been used to explore their impact on stellar model calculations for the weak *s* process in a 25-$M_\odot$ star, which were performed with the post-processing code described in Raiteri et al. (1991) and Käppeler et al. (1994). It was found in these calculations that the nucleosynthesis yields for the weak *s* process show large variations due to the uncertainties of the involved neutron capture cross sections (Heil et al. 2008a). Unlike in the main *s* process, flow equilibrium is not reached during the weak *s* process. Therefore, the neutron capture cross sections do not only influence the yield of the respective isotope, but also the production of all heavier nuclei on the reaction path of the weak *s* process. The impact of the improved MACS described here are illustrated in Figure 3.

The range of uncertainties, which are caused by the extrapolation from the measured energy at $kT = 25$ keV to the higher energies around $kT = 90$ keV are in some cases very large. To improve this situation, complementary new accurate TOF measurements are clearly needed in the mass region $56 \leq A \leq 70$. Accordingly, one has to conclude that reliable abundance predictions for the weak *s* process are only possible if all neutron capture cross sections of the involved isotopes are known with high accuracy. Also the abundant light isotopes below Fe are important, since they may constitute crucial neutron poisons for the *s* process.

Acknowledgments

We are thankful to D. Roller, E.-P. Knaetsch, and W. Seith for their support during the measurements. M.P. and R.G. acknowledge support by the Italian MIUR-PRIN06 Project 'Late phases of Stellar Evolution: Nucleosynthesis in Supernovae, AGB stars, Planetary Nebulae'. M.P. is supported by the Marie Curie Int. Reintegr. Grant MIRG-CT-2006-046520 within the European FP6, and by NSF grants PHY 02-16783 (JINA).

References

Anders, E. & Grevesse, N., 1989, GeCoA, 53, 197
Arlandini, C., Käppeler, F., Wisshak, K., Gallino, R., Lugaro, M., Busso, M. & Straniero, O., 1999, ApJ, 525, 886
Bao, Z. Y., Beer, H., Käppeler, F., Voss, F., Wisshak, K. & Rauscher, T., 2000, ADNDT, 76, 70
Beer, H. & Käppeler, F., 1980, PhRvC, 21, 534
Burbidge, E. M., Burbidge, G. R., Fowler, W. A. & Hoyle, F., 1957, RvMP, 29, 547
Burrows, T. W., 1995, NDS, 74, 1
Chunmei, Z., 2002, NDS, 95, 59
Fröhlich, C., Martínez-Pinedo, G., Liebendörfer, M., Thielemann, F.-K., Bravo, E., Hix, W. R., Langanke, K. & Zinner, N. T., 2006, PhRvL, 96, 142502
Heil, M., Käppeler, F., Uberseder, E., Gallino, R. & Pignatari, M., 2008b, PhRvC, 77, 015808
Heil, M., Käppeler, F., Uberseder, E., Gallino, R., Bisterzo, S. & Pignatari, M., 2008a, PhRvC, 78, 025802
Helmer, R. G., 1994, NDS, 72, 83
Helmer, R. G., 1998, NDS, 83, 285
Käppeler, F., Walter, G. & Mathews, G., 1985, ApJ, 291, 319

https://doi.org/10.1071/AS08064 Published online by Cambridge University Press

Käppeler, F. et al., 1994, ApJ, 437, 396
Katakura, J., 1999, NDS, 86, 955
Kenny, M., Allen, B. J. & Macklin, R. L., 1977, AuJPh, 30, 605
Macklin, R. L., 1984, NSE, 88, 129
Mohr, P., Sedyshev, P. V., Beer, H., Stadler, W., Oberhummer, H., Popov, Yu. P. & Rochow, W., 1999, PhRvC, 59, 3410
Musgrove, A. R. de L., Allen, B. J. & Macklin, R. L., 1978, in Neutron Physics and Nuclear Data for Reactors and other Applied Purposes (Paris: OECD), 426
Nassar, H. et al., 2005, PhRvL, 94, 092504
Pignatari, M., Gallino, R., Meynet, G., Hirschi, R., Herwig, F. & Wiescher, M., 2008, ApJ, 687, L95
Raiteri, C. M., Busso, M., Gallino, R. & Picchio, G., 1991, ApJ, 371, 665
Raiteri, C. M., Gallino, R., Busso, M., Neuberger, D. & Käppeler, F., 1993, ApJ, 419, 207
Rauscher, T., Heger, A., Hoffman, R. D. & Woosley, S. E., 2002, ApJ, 576, 323
Reich, C. W., 1994, NDS, 71, 709
Reich, C. W. & Helmer, R. G., 2000, NDS, 90, 645
Singh, B. & Cameron, J. A., 2001, NDS, 92, 1
Sneden, C. et al., 2003, ApJ, 591, 936
Straniero, O., Gallino, R., Busso, M., Chieffi, A., Raiteri, C. M., Limongi, M. & Salaris, M., 1995, ApJ, 440, L85
The, L.-S., El Eid, M. & Meyer, B., 2007, ApJ, 655, 1058
Travaglio, C., Gallino, R., Arnone, E., Cowan, J., Jordan, F. & Sneden, C., 2004, ApJ, 601, 864
Uberseder, E., Heil, M., Käppeler, F., Görres, J. & Wiescher, M., 2007, PhRvC, 75, 0358019
Walter, G., Beer, H., Käppeler, F., Reffo, G. & Fabbri, F., 1986, A&A, 167, 186
Wu, S.-C., 2000, NDS, 91, 1
Zinner, E., 1998, AREPS, 26, 147

https://doi.org/10.1071/AS08064 Published online by Cambridge University Press